Bifurcation for Dynamical Systems of Planet-Belt Interaction

Ing-Guey Jiang[1] and Li-Chin Yeh[2]

[1] Institute of Astronomy,

National Central University, Chung-Li, Taiwan

[2] Department of Mathematics,

National Hsinchu Teachers College, Hsin-Chu, Taiwan

Received ____________________; accepted ____________________

ABSTRACT

The dynamical systems of planet-belt interaction are studied by the fixed-point analysis and the bifurcation of solutions on the parameter space is discussed. For most cases, our analytical and numerical results show that the locations of fixed points are determined by the parameters and these fixed points are either structurally stable or unstable. In addition to that, there are two special fixed points: the one on the inner edge of the belt is asymptotically stable and the one on the outer edge of the belt is unstable. This is consistent with the observational picture of Asteroid Belt between the Mars and Jupiter: the Mars is moving stablely close to the inner edge but the Jupiter is quite far from the outer edge.

1. Introduction

The discovered number of extra-solar planets is increasing dramatically due to astronomers' observational effort, therefore the dynamical study in this field is getting important. Because the belts of planetesimals often exist among planets within a planetary system as we have in the Solar System, it is indeed important to understand the solutions of dynamical systems of planet-belt interaction. Jiang & Ip [2001] predicted that the interaction with the belt or disc might bring the planetary system of upsilon Andromedae to the current orbital configuration.

Yeh & Jiang [2001] used phase-plane analysis to study the orbital migration problem of scattered planets. They completely classify the parameter space and solutions and conclude that the eccentricity always increases if the planet, which moves on circular orbit initially, is scattered to migrate outward. These analytical results is consistent with the numerical simulations in Thommes, Duncan & Levison [1999].

In addition to astronomy, general or Newton's dynamical systems are studied in many other fields and have very important applications. Clausen et al. [1998] studied periodic modes of motion of a few body system of magnetic holes both experimentally and numerically. Kaulakys et al. [1999] showed that a systems of many bodies moving with friction can experience a transition to chaotic behavior.

On the other hand, Chan et al. [2001] studied bifurcation for limit cycles of quadratic systems interestingly. Similar type of approach should be also good for the bifurcation of solutions for dynamical systems of planet-belt interaction. In this paper, we focus on the planet-belt interaction and study the bifurcation of such system by phase plane analysis.

Basicly, we would like to understand the orbital evolution of a planet which moves around a central star and interacts with a belt. The belt is a annulus with inner radius r_1

and outer radius r_2, where r_1 and r_2 are assumed to be constants. We set $r_1 = 3$ and $r_2 = 6$ for all numerical results in this paper.

We assume the distance between the central star and the planet is r, where r is a function of time. When $r < r_1$, the belt would only give the force which pulls the planet away from the central star. When $r > r_2$, the belt would only give the force which pushes the planet towards the central star. When $r_1 \leq r \leq r_2$, in addition to the usual gravitational force, there is friction between the planet and the belt. These three cases will be studied in Model A ($r < r_1$), Model B($r > r_2$) and Model C($r_1 < r < r_2$) individually.

We will mention our basic governing equations in Section 2. In Section 3-5, we study the locations and stabilities of fixed points by phase plane analysis for Model A, B and C. The conclusions will be in Section 6.

2. The Model

In general, the equation of motion of the planet is (Goldstein 1980)

$$\frac{d^2u}{d\theta^2} = -u - \frac{mf\left(\frac{1}{u}\right)}{l^2u^2}, \tag{1}$$

where $u = 1/r$, m, l are the mass and the angular momentum of the planet and f is the total force acting on the planet. We use the polar coordinate (r, θ) to describe the location of the planet.

The total force f includes the contribution from the central star and the belt. The force from the central star is

$$f_s = -\frac{Gm}{r^2}, \tag{2}$$

where we have set the mass of the central star to be one. If the density profile of belt is $\Sigma(r) = c_0/r$ where c_0 is a constant completely determined by the total mass of the belt.

The total mass of the belt is

$$M_{b0} = \int_0^{2\pi} \int_{r_1}^{r_2} \Sigma(r')r'dr'd\phi = 2\pi c_0(r_2 - r_1) \tag{3}$$

In general, the force from the belt for the planet is complicated and involved the Elliptic Integral. We use a simpler integral to over-estimate the force and then use a small number $0 < \beta < 1$ to correct the force approximately.

When the planet is not within the belt region, the force from the belt is

$$\begin{aligned} f_{b\pm} &= \pm\beta \int_{-\pi}^{\pi} \int_{r_1}^{r_2} \frac{Gm\Sigma(r')r'}{r^2 + (r')^2 - 2rr'\cos\phi} dr'd\phi \\ &= \pm\frac{\beta\pi G c_0 m}{r} \left\{ \ln \left| \frac{(r_1 - r)(r + r_2)}{(r_2 - r)(r + r_1)} \right| \right\} \\ &= \pm\frac{\pi G c m}{r} \left\{ \ln \left| \frac{(r_1 - r)(r + r_2)}{(r_2 - r)(r + r_1)} \right| \right\}, \end{aligned} \tag{4}$$

where $+$ stands for the case when $r < r_1$ (the belt pulls the planet away from the central star), $-$ stands for the case when $r > r_2$ (the belt pushes the planet towards the central star) and we define $c = \beta c_0$.

When the planet is within the belt region, the gravitational force from the belt is

$$\begin{aligned} f_{b\epsilon} &= -\beta \int_{-\pi}^{\pi} \int_{r_1}^{r-\epsilon} \frac{Gm\Sigma(r')r'}{r^2 + (r')^2 - 2rr'\cos\phi} dr'd\phi + \beta \int_{-\pi}^{\pi} \int_{r+\epsilon}^{r_2} \frac{Gm\Sigma(r')r'}{r^2 + (r')^2 - 2rr'\cos\phi} dr'd\phi, \\ &= \frac{\pi G c m}{r} \ln \left\{ \left| \frac{(r + r_1)(r + r_2)}{(r - r_1)(r - r_2)} \right| \left(\frac{\epsilon^2}{4r^2 - \epsilon^2} \right) \right\}, \end{aligned} \tag{5}$$

where ϵ is a small number to avoid the singularity of the integral. To be convenient, we define the effective mass of the belt to give force on the planet to be

$$M_b \equiv \beta M_{b0} = 2\pi c(r_2 - r_1). \tag{6}$$

Because there might be some scattering between the planetesimals in the belt and the planet, we should include frictional force in this case. This frictional force should be

proportional to the surface density of the belt at the location of the planet and the velocity of the planet. However, if the planet is doing circular motion, the probability of close encounter between the planet and the planetesimals in the belt is very small and can be neglect here. Thus, we can assume that the frictional force is proportional to the radial velocity of the planet dr/dt only and ignore the $d\theta/dt$ dependence.

Therefore, f_α is proportional to the surface density of the belt and radial velocity dr/dt. Hence, we write down the formula for frictional force as

$$f_\alpha = -\alpha\Sigma(r)\frac{dr}{dt} = -\frac{\alpha c}{r}\frac{dr}{dt}, \tag{7}$$

where α is a frictional parameter. Because the $d\theta/dt$ component of the planetary velocity is ignored in the frictional force, the angular momentum l is conserved here, so we have

$$mr^2 d\theta = l dt. \tag{8}$$

Because of this, we can use θ as our independent variable. We use θ to label time t afterward and one can easily gets t from the above equation.

Since $u = 1/r$ and equation (8), we have

$$\frac{dr}{dt} = \frac{dr}{d\theta}\frac{d\theta}{dt} = \frac{l}{mr^2}\frac{dr}{d\theta} = -\frac{l}{m}\frac{du}{d\theta}. \tag{9}$$

Equation (7) becomes

$$f_\alpha = \frac{l\alpha c u}{m}\frac{du}{d\theta}. \tag{10}$$

3. Model A

In this model, we assume that the star-planet distance is less than the inner radius of the belt, i.e. $r < r_1$. Thus, $f = f_s + f_{b+}$, where f_s and f_{b+} are defined in Section 2. Since $r < r_1 < r_2$, from equation (4), we have

$$f_{b+} = \frac{\pi G c m}{r} \left\{ \ln \left| \frac{(r_1 - r)(r + r_2)}{(r_2 - r)(r + r_1)} \right| \right\}.$$

We further define that $u \equiv 1/r$ and also

$$P_I(u) \equiv \left| \frac{(r_1 u - 1)(1 + r_2 u)}{(r_2 u - 1)(1 + r_1 u)} \right|. \tag{11}$$

We can then transform equation (1) into

$$\frac{d^2 u}{d\theta^2} = -u + \frac{Gm^2}{l^2} - \frac{\pi G c m^2}{l^2 u} \left\{ \ln P_I(u) \right\}. \tag{12}$$

Therefore, the equation of motion for this system can be written as

$$\frac{du}{d\theta} = v \tag{13}$$

$$\frac{dv}{d\theta} = -u + k_2 - \frac{k_3}{u} \ln(P_I(u)), \tag{14}$$

where $k_2 = Gm^2/(l^2)$ and $k_3 = (c\pi G m^2)/(l^2)$.

3.1. Fixed Points for Model A

The fixed points (u, v) of problem (3) satisfy the following equations

$$v = 0$$

$$\text{and} \qquad -u + k_2 - \frac{k_3}{u} \ln(P_I(u)) = 0. \tag{15}$$

Obviously, only those solutions locating in the region that $u > 1/r_1$ have physical meaning since we consider the case that $r < r_1$ is this model. However, the properties of the

fixed points in unphysical region would affect the topology of the solution curves in physical region, so we have to study fixed points both in physical and unphysical regions.

If we define

$$Q_A(u) = \exp\left\{-\frac{u^2}{k_3} + \frac{k_2}{k_3}u\right\}, \tag{16}$$

from equation (15), we know that fixed points should satisfy $P_I(u) = Q_A(u)$. In the following theorem, we prove that there are at least three fixed points in whole phase space and at least one locates within the physical region, $u > 1/r_1$.

In our theorems, we denote $(1/r_1)^+$ to represent that u tends to $1/r_1$ from the right hand side and $(1/r_1)^-$ to represent that u tends to $1/r_1$ from the left hand side etc.

Theorem 3.1

(a) There is at least one $u_* < 1/r_2$ such that $P_I(u_*) = Q_A(u_*)$.

(b) There is at least one $u_{**} \in (1/r_2, 1/r_1)$ such that $P_I(u_{**}) = Q_A(u_{**})$.

(c) There is at least one $u_{***} > 1/r_1$ such that $P_I(u_{***}) = Q_A(u_{***})$.

Proof :

Let $R_A(u) \equiv P_I(u) - Q_A(u)$, where $P_I(u)$ and $Q_A(u)$ are defined in equation (11) and equation (16).

(a) Since

$$R'_A(u) = \frac{2(r_2 - r_1)(1 + r_1 r_2 u^2)}{[1 - (r_2 - r_1)u - r_1 r_2 u^2]^2} - \exp\left\{-\frac{u^2}{k_3} + \frac{k_2}{k_3}u\right\}\left\{-\frac{2u}{k_3} + \frac{k_2}{k_3}\right\},$$

we have

$$R'_A(0) = 2(r_2 - r_1) - \frac{k_2}{k_3} = 2(r_2 - r_1) - \frac{1}{\pi c} = 2(r_2 - r_1) - \frac{2(r_2 - r_1)}{M_b} = 2(r_2 - r_1)\left(1 - \frac{1}{M_b}\right). \tag{17}$$

Because the total mass of the belt is assumed to be less than the mass of the central star,

i.e. $0 < M_b < 1$, we have $R'_A(0) < 0$. Since $R_A(0) = 0$, $R'_A(0) < 0$, and $R_A\left((1/r_2)^-\right) > 0$, we have that there exists $u_* \in (0, 1/r_2)$ such that $R_A(u_*) = 0$, that is, $P_I(u_*) = Q_A(u_*)$.□

(b) Since $R_A\left((1/r_2)^+\right) > 0$ and $R_A((1/r_1)^-) < 0$, we have that there exists $u_{**} \in (1/r_2, 1/r_1)$ such that $R_A(u_{**}) = 0$, that is, $P_I(u_{**}) = Q_A(u_{**})$.□

(c) In the region of $u > 1/r_1$, we have $R_A(1/r_1) = P_I(1/r_1) - \exp\left\{-\frac{r_1^2}{k_3} + \frac{k_2}{k_3} r_1\right\} < 0$.

Further, because $\exp\left\{-\frac{u^2}{k_3} + \frac{k_2}{k_3} u\right\} \to 0$ as $u \to \infty$, $P_I(u) \to 1$ as $u \to \infty$ and $R_A(u) \to 1$ as $u \to \infty$, there is a $u_{***} > 1/r_1$ such that $R_A(u_{***}) = 0$, i.e. $P_I(u_{***}) = Q_A(u_{***})$.□

Figure 1(a)-(b) are the numerical results for the solutions of equation (15). That is, we find all possible fixed points u for any given k_2 and M_b with fixed values of r_1 and r_2. Figure 1(a) are the results on $k_2 - u$ plane, where dashed lines are for $M_b = 0.1$, dotted lines are for $M_b = 0.5$ and solid lines are for $M_b = 1.0$. There are three lines for each value of M_b but only two solid lines can be seen because one solid line overlaps with the k_2-axis. Thus, there are three fixed points for any given values of k_2 and M_b. Figure 1(b) are the results on $M_b - u$ plane, where dashed lines are for $k_2 = 0.1$, dotted lines are for $k_2 = 0.5$ and solid lines are for $k_2 = 1.0$.

From these results, we can completely determine the locations of fixed points for different values of k_2 and M_b, where we assume $0 < k_2 < 1$ and $0 < M_b < 1$. These results are consistent with the analytic results of Theorem 3.1.

3.2. Phase-Planes for Model A

Following the linearization analysis, the eigenvalues λ corresponding to the fixed points (u, v) satisfy the following equation

$$\lambda^2 - (-1 - k_3 \frac{\partial A_1}{\partial u}) = 0,$$

where $A_1 = (\ln P_I(u))/(u)$, so

$$\frac{\partial A_1}{\partial u} = -\frac{\ln P_I(u)}{u^2} + \frac{1}{uP_I(u)} \frac{\partial P_I(u)}{\partial u} \tag{18}$$

Hence

$$\lambda = \pm\sqrt{-1 - k_3 \frac{\partial A_1}{\partial u}}. \tag{19}$$

We thus have two cases in the following:

Case 1: If $-1 - k_3 \frac{\partial A_1}{\partial u} > 0$, then λ are real with opposite sign, so in this case, the fixed point is a unstable saddle point.

Case 2 : If $-1 - k_3 \frac{\partial A_1}{\partial u} < 0$, then λ are pure complex numbers with opposite sign, so in this case, the fixed point is a center point.

Although we understand that when the real parts of the eigenvalues of a fixed point equal to zero in the first-order linearization analysis, the properties of this fixed point should be determined by the higher order analysis in general. However, to simply our language, we still use the term, center point, for any fixed point with zero real parts of eigenvalues. This is a good choice because our numerical results show that these points are in fact center points.

In the following theorem, we discuss the properties of the fixed point for the physical region, i.e. $u > 1/r_1$.

Theorem 3.2

If the fixed point $u^* > 1/r_1$, then this fixed point u^* is a center point.

Proof :

First, from equation (15) and equation (18), we calculate

$$\begin{aligned} -1-k_3\frac{\partial A_1}{\partial u} &= -1+k_3\frac{\ln P_I(u)}{u^2}-\frac{2k_3(r_2-r_1)(1+r_1r_2u^2)}{u(r_2^2u^2-1)(r_1^2u^2-1)} \\ &= -1+k_3\left(-\frac{1}{k_3}+\frac{k_2}{k_3}\frac{1}{u}\right)-\frac{2k_3(r_2-r_1)(1+r_1r_2u^2)}{u(r_2^2u^2-1)(r_1^2u^2-1)} \\ &= -2+\frac{k_2}{u}-\frac{2k_3(r_2-r_1)(1+r_1r_2u^2)}{u(r_2^2u^2-1)(r_1^2u^2-1)}. \end{aligned} \tag{20}$$

For the convenience, we separate the proof into two parts:

(i) when $k_2/2 < 1/r_1$:

Since $u^* > 1/r_1$, we have $u^* > k_2/2$. Thus, $-2+k_2/u^* < 0$, so $-1-k_3\frac{\partial A_1}{\partial u}\Big|_{u=u^*} < 0$. The fixed point u^* is therefore a center point.

(ii) when $k_2/2 > 1/r_1$:

Since $u^* > 1/r_1$ is a fixed point, u^* satisfy $P_I(u^*) = Q_A(u^*)$. Since we consider the region $u > 1/r_1$, we have

$$0 < P_I(u) < 1 \text{ for } u > 1/r_1 \tag{21}$$

Moreover, because Q_A only has one critical point at $u = k_2/2$, i.e. $Q'_A(k_2/2) = 0$ and $Q''_A(k_2/2) < 0$, $Q_A(k_2/2)$ is a global maximum and

$$Q_A\left(\frac{k_2}{2}\right) > Q_A(k_2) = 1.$$

Since $Q_A(0) = 1$, $Q_A(k_2/2) > 1$ and $Q''_A(u) < 0$ for $u < k_2$, we have $Q_A(u) \geq 1$ for $u < k_2$. From equation (21), we have $R_A(k_2) = P_I(k_2) - Q_A(k_2) < 0$ and $\lim_{u\to\infty} R_A(u) = 1$. Therefore, we have $u^* > k_2$.

Because $u^* > k_2/2$, we have $-2+k_2/u^* < 0$ and thus $-1-k_3\frac{\partial A_1}{\partial u} < 0$. Therefore, the fixed point u^* is a center point.□

The solution curves on the $u-v$ phase plane are shown in Figure 1(c)-(d), where we set $k_2 = 0.2$, $M_b = 0.3$. In Figure 1(c), there are two vertical dotted lines, the left one is

$u = 1/r_2$ and the right one is $u = 1/r_1$, which divide the $u - v$ plane into three regions. It is obvious that there is one fixed point in each region, which is consistent with Theorem 3.1 and the fixed point in the region of $u > 1/r_1$ is a center point, which is precisely what we have proved in Theorem 3.2. Figure 1(d) is just the detail of the solution curves near this fixed point in the region of $u > 1/r_1$. These figures reconfirm the analytic results and also make the behavior of the solution curve clear. We thus have known the behavior of the solutions completely.

4. Model B

In this model, we assume that the star-planet distance is larger than the outer radius of the belt, i.e. $r > r_2$. Thus, $f = f_s + f_{b-}$, where f_s and f_{b-} are defined in Section 2. (f_s is defined by equation (2) and f_{b-} is defined by equation (4).)

In this model, since $r > r_2 > r_1$, from equation (4) in Section 2, we have

$$f_{b-} = -\frac{\pi G c m}{r}\left\{\ln\left|\frac{(r_1 - r)(r + r_2)}{(r_2 - r)(r + r_1)}\right|\right\}.$$

By $u = 1/r$ and equation (1), we have the equation of motion:

$$\frac{d^2u}{d\theta^2} = -u + \frac{Gm^2}{l^2} + \frac{\pi G c m^2}{l^2 u}\left\{\ln\left|\frac{(1 - r_1 u)(1 + r_2 u)}{(1 - r_2 u)(1 + r_1 u)}\right|\right\}. \tag{22}$$

Similarly, we set $k_2 = Gm^2/(l^2)$ and $k_3 = (c\pi Gm^2)/(l^2)$ and transform equation (22) to the following problem:

$$\frac{du}{d\theta} = v \tag{23}$$

$$\frac{dv}{d\theta} = -u + k_2 + \frac{k_3}{u}\ln(P_I(u)), \tag{24}$$

where $P_I(u)$ is defined in equation (11).

4.1. Fixed Points for Model B

The fixed points (u, v) of problem (4) satisfy the following equations

$$v = 0$$

$$\text{and} \qquad -u + k_2 + \frac{k_3}{u}\ln(P_I(u)) = 0. \tag{25}$$

If we define

$$Q_B(u) \equiv \exp\left\{\frac{u^2}{k_3} - \frac{k_2}{k_3}u\right\}, \tag{26}$$

and

$$R_B(u) \equiv P_I(u) - Q_B(u), \tag{27}$$

then fixed points $(u, 0)$ should satisfy $R_B(u) = 0$. In the following theorem, we discuss the properties of fixed points in different parameter space.

Theorem 4.1

For convenience, we define three regions as:

Region (I): $u < 1/r_2$ (this is the physical region for Model B),

Region (II): $1/r_2 < u < 1/r_1$,

Region (III): $u > 1/r_1$.

(a) In Region (I), if $k_2 > 1/r_2$, then there is no fixed point in this $u < 1/r_2$ region.

(b) In Region (II), there is at least one fixed point.

(c) In Region (III), if $k_2 < 1/r_1$, then there is no fixed point.

(d) Within Region (III), if $1/r_1 < k_2/2$ and $P_I(k_2/2) > Q_B(k_2/2)$, then there is one unique fixed point: $u_2 \in (1/r_1, k_2/2)$ and at least one fixed point $u_3 \in (k_2/2, k2)$.

(e) Within Region (III), if $1/r_1 < k_2/2$ and $P_I(k_2/2) < Q_B(k_2/2)$, then there is no fixed point in the region of $(1/r_1, k_2/2)$.

(f) In Region (III), if $1/r_1 < k_2/2$ and $P_I'(u) > Q_B'(u)$ for $u \in (k_2/2, k_2)$, then there is no fixed point.

Proof :

From the definition of $Q_B(u)$ in equation (26), we have $Q_B'(k_2/2) = 0$ and $Q_B''(u) > 0$ for all u. Thus, Q_B only has one critical point at $k_2/2$ and $Q_B(k_2/2)$ is a global minimum.

Moreover, because $Q_B(0) = 1 = Q_B(k_2)$, we have

$$Q_B(u) < 1 \text{ for } u \in (0, k_2); \tag{28}$$

$$Q_B(u) > 1 \text{ for } u \in (k_2, \infty). \tag{29}$$

(a) Since $P_I(0) = 0$ and $P_I'(u) > 0$, we have

$$P_I(u) > 1 \text{ for } u \in \left(0, \frac{1}{r_2}\right). \tag{30}$$

Because of the condition $k_2 > 1/r_2$, from equation (28), we have

$$Q_B(u) < 1 \text{ for } u \in \left(0, \frac{1}{r_2}\right). \tag{31}$$

From equation (30) and (31), we have $R_B(u) = P_I(u) - Q_B(u) > 0$ for $u < 1/r_2$. Therefore, there is no fixed point in this physical region, $u < 1/r_2$.□

(b) Because $R_B((1/r_2)^+) > 0$ and $R_B(1/r_1) = -\exp\{r_1^2/k_3 - k_2/k_3\} < 0$, there is at least one $u_1 \in (1/r_2, 1/r_1)$ such that $R_B(u_1) = 0$. □

(c) Because of the condition $k_2 < 1/r_1$, from equation (29), we have

$$Q_B(u) > 1 \text{ for } u \in \left(\frac{1}{r_1}, \infty\right). \tag{32}$$

Since $P_I(1/r_1) = 0$, $P_I'(u) > 0$ and $\lim_{u\to\infty} P_I(u) = 1$, we have

$$0 < P_I(u) < 1 \text{ for } u \in \left(\frac{1}{r_1}, \infty\right). \tag{33}$$

From equation (32) and (33), we have $R_B(u) = P_I(u) - Q_B(u) < 0$ for all $u \in (1/r_1, \infty)$. Therefore, there is no fixed point in this case. □

(d) In the region of $(1/r_1, k_2/2)$, we have $R_B(1/r_1) < 0$, $R_B'(u) = P_I'(u) - Q_B'(u) > 0$ and from our assumption $R_B(k_2/2) = P_I(k_2/2) - Q_B(k_2/2) > 0$, so there is one unique fixed point $u_2 \in (1/r_1, k_2/2)$. Because $R_B(k_2) < 0$ and $R_B(k_2/2) > 0$, there is at least one fixed point $u_3 \in (k_2/2, k_2)$. □

(e) Because $R_B(1/r_1) < 0$, $R_B'(u) = P_I'(u) - Q_B'(u) > 0$ for $u \in (1/r_1, k_2/2)$ and from our assumption $R_B(k_2/2) = P_I(k_2/2) - Q_B(k_2/2) < 0$, there is no fixed point in this $(1/r_1, k_2/2)$ region. □

(f) First, we consider the region of $(1/r_1, k_2)$. Because of the condition $1/r_1 < k_2/2$ and $R_B'(u) = P_I'(u) - Q_B'(u) > 0$ for $u \in (k_2/2, k_2)$, from our assumption, we have

$$R_B'(u) = P_I'(u) - Q_B'(u) > 0 \quad \text{for all } u \in \left(\frac{1}{r_1}, k_2\right).$$

Further, since $R_B(1/r_1) < 0$ and $R_B(k_2) < 0$, there is no fixed point in $(1/r_1, k_2)$. Secondly, we consider the region of (k_2, ∞). Because $P_I(u) \leq 1$, $Q_B(u) > Q_B(k_2) = 1$ and thus $R_B(u) = P_I(u) - Q_B(u) < 0$ for all $u > k_2$, so there is no fixed point in (k_2, ∞) region. Therefore, from the above two, we have proved that there is no fixed point in the region of $(1/r_1, \infty)$. □

In Theorem 4.1(a), we did not discuss the case when $k_2 < 1/r_2$. In Figure 2(a), we plot R_B as function of u for the cases that $M_b = 0.5$ and $k_2 = 0.02$ (solid line), $k_2 = 0.04$

(dotted line), $k_2 = 0.06$ (dashed line), $k_2 = 0.08$ (long dashed line). All these values of k_2 satisfy $k_2 < 1/r_2$. It is obvious that there is no root for $k_2 = 0.08$ (long dashed line) and two roots for others. From these numerical results, we know that there could be two fixed points or no fixed point in the $(0, 1/r_2)$ region if $k_2 < 1/r_2$.

On the other hand, in Theorem 4.1(c)-(f), we did not discuss the case when $k_2/2 < 1/r_1 < k_2$. In Figure 2(b), we plot R_B as function of u for the cases that $M_b = 0.5$ and $k_2 = 0.4$ (solid line), $k_2 = 0.5$ (dotted line), $k_2 = 0.6$ (dashed line). All these values of k_2 satisfy $k_2/2 < 1/r_1 < k_2$. It is obvious that there is no root for $k_2 = 0.4$ (solid line) and two roots for others. From these numerical results, we found that there could be two fixed points or no fixed point in in Region (III), i.e. $(1/r_1, \infty)$ if $k_2/2 < 1/r_1 < k_2$.

Figure 2(c)-(d) are the numerical results for the solutions of equation (25). That is, we find all possible fixed points u for any given k_2 and M_b with fixed values of r_1 and r_2.

Figure 2(c) are the results on $k_2 - u$ plane, where dashed lines are for $M_b = 0.1$, dotted lines are for $M_b = 0.5$ and solid lines are for $M_b = 1.0$. From this figure, we know that there are three fixed points when k_2 is closer to 0 or 1, i.e. the left or right side of the figure. However, there could be one fixed point only in the middle. Figure 2(d) are the results on $M_b - u$ plane, where dashed lines are for $k_2 = 0.1$, dotted lines are for $k_2 = 0.5$ and solid lines are for $k_2 = 1.0$.

Checking the detail of these figures and Theorem 4.1, we found that they are completely consistent with each other.

4.2. Phase-Planes for Model B

To study the phase planes, we need to know the eigenvalues of every fixed point. The eigenvalues λ corresponding to a fixed point (u, v) satisfy the following equation:

$$\lambda^2 - (-1 + k_3 \frac{\partial B_1}{\partial u}) = 0,$$

$$\text{where} \qquad \frac{\partial B_1}{\partial u} = \frac{\partial[\ln(P_I(u))/u]}{\partial u} = -\frac{\ln P_I(u)}{u^2} + \frac{1}{uP_I(u)} \frac{\partial(P_I(u))}{\partial u} \tag{34}$$

Hence

$$\lambda = \pm\sqrt{-1 + k_3 \frac{\partial B_1}{\partial u}}. \tag{35}$$

We have two cases for the eigenvalues in the following:

Case 1: If $-1 + k_3 \frac{\partial B_1}{\partial u} > 0$, then λ are real with opposite sign, so the fixed point is a unstable saddle point.

Case 2: If $-1 + k_3 \frac{\partial B_1}{\partial u} < 0$, then λ are pure complex numbers with opposite sign, so the fixed point is a center point.

Theorem 4.2

If $k_2 r_2 < 2$, then there is a unique fixed point $u_1 \in (1/r_2, 1/r_1)$ and this fixed point is a center point.

Proof :

Since fixed point (u, v) satisfy equation (25), from equation (34), we have

$$\begin{aligned} -1 + k_3 \frac{\partial B_1}{\partial u} &= -1 + k_3 \left\{ -\frac{\ln P_I(u)}{u^2} + \frac{2}{u} \frac{(r_2 - r_1)(1 + r_1 r_2 u^2)}{(1 - r_2^2 u^2)(1 - r_1^2 u^2)} \right\} \\ &= -1 + k_3 \left\{ -\frac{1}{k_3} + \frac{k_2}{k_3 u} + \frac{2}{u} \frac{(r_2 - r_1)(1 + r_1 r_2 u^2)}{(1 - r_2^2 u^2)(1 - r_1^2 u^2)} \right\} \\ &= -2 + \frac{k_2}{u} + \frac{2k_3}{u} \frac{(r_2 - r_1)(1 + r_1 r_2 u^2)}{(1 - r_2^2 u^2)(1 - r_1^2 u^2)} \\ &= -2 + \frac{k_2}{u} - \frac{k_2 M_b (1 + r_1 r_2 u^2)}{u(r_2^2 u^2 - 1)(1 - r_1^2 u^2)}. \end{aligned} \tag{36}$$

Since $k_2/2$ is a global minimum of $Q_B(u)$ and $k_2/2 < 1/r_2$, we know that $Q'_B(u) > 0$ for $u \in (1/r_2, 1/r_1)$. Because $P'_I(u) < 0$ and $Q'_B(u) > 0$ for all $u \in (1/r_2, 1/r_1)$, we have

$R_B'(u) = P_I'(u) - Q_B'(u) < 0$ for all $u \in (1/r_2, 1/r_1)$. Moreover, it can be shown that $R_B((1/r_2)^+) = \infty$ and $R_B(1/r_1) = -Q_B(1/r_1) < 0$, thus there is a unique fixed point $u_1 \in (1/r_2, 1/r_1)$ such that $R_B(u_1) = 0$.

Because this fixed point $u_1 \in (1/r_2, 1/r_1)$, we have

$$-2 + \frac{k_2}{u_1} < -2 + k_2 r_2 < 0.$$

Since the third term of equation (36) is always negative, we have $-1 + k_3 \frac{\partial B_1}{\partial u}\Big|_{u=u_1} < 0$. Therefore, this fixed point is a center point. □

The solution curves on the $u - v$ phase plane are shown in Figure 3(a)-(d), where the vertical dotted lines are $u = 1/r_2$ and $u = 1/r_1$. Figure 3(a) is the result when $k_2 = 0.05$, $M_b = 0.5$, which corresponds to the left region of Figure 2(c) (on the dotted line and k_2 is closer to 0). Thus, there are three fixed points: one is larger than $1/r_2$ and others are less than $1/r_2$. Figure 3(b) is the result when $k_2 = 0.8$, $M_b = 0.5$, which corresponds to the right region of Figure 2(c) (on the dotted line and k_2 is closer to 1). Thus, there are three fixed points: one is less than $1/r_1$ and others are larger than $1/r_1$. Figure 3(c) is the result when $k_2 = 0.5$, $M_b = 0.5$, which corresponds to the middle region of Figure 2(c) (on the dotted line and about the region between 0.08 and 0.55) Thus, there is only one fixed point. Figure 3(d) is the result when $k_2 = 1.0$, $M_b = 0.8$, which corresponds to the right region of solid lines in Figure 2(d). Since M_b is closer to 1, there are three fixed points: one is less than $1/r_1$ and others are larger than $1/r_1$. Therefore, the numbers of fixed points in Figure 3 are in fact completely consistent with Figure 2.

Figure 3(a), 3(c) and 3(b) give us a chance to see the transition of phase plane along the dotted line in Figure 2(c) from left side to the right side. In Figure 3(a), there are one center and one saddle point in the region of $u < 1/r_2$ and one center in the region of $1/r_2 < u < 1/r_1$. However, in Figure 3(c), the left two fixed points disappear, so there is only one fixed point, which is the center in the region of $1/r_2 < u < 1/r_1$. Moreover, the

shape of the solution curves in the region of $u > 1/r_1$ already become different from the curves close to a center. Finally, in Figure 3(b), there is still one center point in the region of $1/r_2 < u < 1/r_1$ but there are two new fixed points: one saddle and one center in the region of $u > 1/r_1$. The locations of these bifurcation points, where transitions of phase plane occur, can be easily seen from Figure 2(c).

These figures reconfirm the analytic results and also make the behavior of the solution curves clear.

5. Model C

In this model, we assume that the star-planet distance is between the inner and outer radius of the belt, i.e $r_1 < r < r_2$. Thus, $f = f_s + f_\alpha + f_{b\epsilon}$ where f_s, f_α and $f_{b\epsilon}$ are defined in Section 2.

From equation (1), set $u = 1/r$, we have

$$\frac{d^2u}{d\theta^2} = -u + \frac{Gm^2}{l^2} - \frac{\alpha c}{lu}\frac{du}{d\theta} - \frac{\pi Gcm^2}{l^2u}\ln\left\{\left|\frac{(1+r_1u)(1+r_2u)}{(1-r_1u)(r_2u-1)}\left(\frac{\epsilon^2u^2}{4-\epsilon^2u^2}\right)\right|\right\}. \tag{37}$$

To simplify the equation, we define

$$P_\epsilon(u) \equiv \left|\frac{(1+r_1u)(1+r_2u)}{(1-r_1u)(r_2u-1)}\left(\frac{\epsilon^2u^2}{4-\epsilon^2u^2}\right)\right|. \tag{38}$$

Hence, equation (37) becomes

$$\frac{d^2u}{d\theta^2} + \frac{k_1}{u}\frac{du}{d\theta} = -u + k_2 - \frac{k_3}{u}\ln(P_\epsilon(u)) \tag{39}$$

where $k_1 = (\alpha c)/l$, $k_2 = (Gm^2)/(l^2)$ and $k_3 = (c\pi Gm^2)(l^2)$. Therefore, we transform equation (39) to the following problem

$$\begin{aligned}
\frac{du}{d\theta} &= v, \\
\frac{dv}{d\theta} &= -u + k_2 - \frac{k_1}{u}v - \frac{k_3}{u}\ln(P_\epsilon(u)).
\end{aligned} \tag{40}$$

5.1. Fixed Points for Model C

The fixed points (u, v) of problem (40) satisfy the following equations

$$v = 0$$

$$\text{and} \qquad -u + k_2 - \frac{k_1}{u}v - \frac{k_3}{u}\ln(P_\epsilon(u)) = 0. \tag{41}$$

We define

$$Q_c(u) \equiv \exp\left\{-\frac{u^2}{k_3} + \frac{k_2}{k_3}u\right\}, \tag{42}$$

and

$$R_c(u) \equiv P_\epsilon(u) - Q_c(u), \tag{43}$$

then the fixed points (u, v) satisfy $R_c(u) = 0$. In the following theorem, we discuss some properties about the fixed points.

Theorem 5.1

(a) There is at least one fixed point $u_1 \in (0, 1/r_2)$.

(b) There is at least one fixed point $u_{\epsilon *} \in (1/r_2, \bar{u})$, where $\bar{u} \in (1/r_2, 1/r_1)$ such that $P'_\epsilon(\bar{u}) = 0$. Moreover,

$$u_{\epsilon *} = \frac{1}{r_2} + \mathrm{O}(\epsilon^2), \text{ so } \lim_{\epsilon \to 0} u_{\epsilon *} = \frac{1}{r_2}. \tag{44}$$

(c) There is at least one fixed point $u_\epsilon^* \in (\bar{u}, 1/r_1)$, where $\bar{u} \in (1/r_2, 1/r_1)$ such that $P_\epsilon'(\bar{u}) = 0$. Moreover,

$$u_\epsilon^* = \frac{1}{r_1} + \mathrm{O}(\epsilon^2), \text{ so } \lim_{\epsilon \to 0} u_\epsilon^* = \frac{1}{r_1}. \tag{45}$$

(d) There are at least two fixed point $u_2, u_3 \in (1/r_1, 2/\epsilon)$.

Proof :

(a) Since $R_c(0) = -Q_c(0) < 0$ and $R_c((1/r_2)^-) > 0$, there is a root $u_1 \in (0, 1/r_2)$ such that $R_c(u_1) = 0$. Thus, u_1 is a fixed point.□

(b) From equation (38), if we consider $u \in (1/r_2, 1/r_1)$, then we have

$$P_\epsilon'(u) = \frac{2\epsilon^2 u}{(1 - r_1 u)(r_2 u - 1)(4 - \epsilon^2 u^2)} \left\{ -\frac{(r_1 + r_2)(1 - r_1 r_2 u^2) u}{(1 - r_1 u)(r_2 u - 1)} + \frac{4(1 + r_1 u)(1 + r_2 u)}{(4 - \epsilon^2 u^2)} \right\}. \tag{46}$$

Since $P_\epsilon'((1/r_2)^+) < 0$, $P_\epsilon'((1/r_1)^-) > 0$ and $P_\epsilon''(u) > 0$ for $u \in (1/r_2, 1/r_1)$, there is a $\bar{u} \in (1/r_2, 1/r_1)$ such that $P_\epsilon'(\bar{u}) = 0$.

Since $P_\epsilon'(\bar{u}) = 0$, from equation (46), we have

$$\frac{(r_1 + r_2)(1 - r_1 r_2 (\bar{u})^2)\bar{u}}{(1 - r_1 \bar{u})(r_2 \bar{u} - 1)} = \frac{4(1 + r_1 \bar{u})(1 + r_2 \bar{u})}{(4 - \epsilon^2 (\bar{u})^2)} \tag{47}$$

Therefore, from equation (47), we have

$$\begin{aligned} P_\epsilon(\bar{u}) &= \frac{(1 + r_1 \bar{u})(1 + r_2 \bar{u})}{(1 - r_1 \bar{u})(r_2 \bar{u} - 1)} \left(\frac{\epsilon^2 (\bar{u})^2}{4 - \epsilon^2 (\bar{u})^2} \right) > 0 \\ &= \frac{4\epsilon^2 \bar{u} (1 + r_1 \bar{u})^2 (1 + r_2 \bar{u})^2}{(4 - \epsilon^2 (\bar{u})^2)^2 (r_1 + r_2)(1 - r_1 r_2 (\bar{u})^2)}. \end{aligned} \tag{48}$$

From equation (48), we have $P_\epsilon(\bar{u}) = \mathrm{O}(\epsilon^2)$.

Since $R_c\left((1/r_2)^+\right) > 0$, and

$$R_c(\bar{u}) = P_\epsilon(\bar{u}) - Q_c(\bar{u}) = \mathrm{O}(\epsilon^2) - Q_c(\bar{u}) < 0, \tag{49}$$

we have that there is at least one fixed point $u_{\epsilon *} \in (1/r_2, \bar{u})$ such that $R_c(u_{\epsilon *}) = 0$.

In the following, we prove that equation (44) holds. Since $R_c(u_{\epsilon *}) = 0$, we have $P_\epsilon(u_{\epsilon *}) = Q_c(u_{\epsilon *})$, that is,

$$\ln\left\{\frac{(1+r_1u_{\epsilon *})(1+r_2u_{\epsilon *})}{(1-r_1u_{\epsilon *})(r_2u_{\epsilon *}-1)}\left(\frac{\epsilon^2u_{\epsilon *}^2}{4-\epsilon^2u_{\epsilon *}^2}\right)\right\} = -\frac{1}{k_3}u_{\epsilon *}^2 + \frac{k_2}{k_3}u_{\epsilon *}. \tag{50}$$

We found the right hand side in equation (50) is bounded for all $\epsilon > 0$, since $u_{\epsilon *} \in (1/r_2, \bar{u})$. We can rewrite the left hand side of equation (50) to be

$$\ln\left\{\frac{1+r_1u_{\epsilon *}}{1-r_1u_{\epsilon *}}\right\} + \ln\left\{\frac{1+r_2u_{\epsilon *}}{4-\epsilon^2u_{\epsilon *}^2}\right\} + \ln\left\{\frac{\epsilon^2u_{\epsilon *}^2}{r_2u_{\epsilon *}-1}\right\}. \tag{51}$$

It is easy to show that the first term and the second term in equation (51) are bounded for all $\epsilon > 0$ since $u_{\epsilon *} \in (1/r_2, \bar{u})$. Therefore, the third term in equation (51) is bounded. That is, there exists a $M > 0$ such that

$$-M < \ln\left\{\frac{\epsilon^2u_{\epsilon *}^2}{r_2u_{\epsilon *}-1}\right\} < M. \tag{52}$$

Since $u_{\epsilon *} \in (1/r_2, \bar{u})$, from equation (52), we have

$$1 + \frac{\epsilon^2}{(1/\bar{u})^2\exp(-M)} < r_2u_{\epsilon *} < 1 + \frac{\epsilon^2r_2^2}{\exp(M)}. \tag{53}$$

Therefore, $u_{\epsilon *} = \frac{1}{r_2} + \mathrm{O}(\epsilon^2)$ and

$$\lim_{\epsilon \to 0} u_{\epsilon *} = \frac{1}{r_2}.\square$$

(c) From equation (49), we have $R_c(\bar{u}) < 0$ and $R_c((1/r_1)^-) > 0$, so there is at least one fixed point $u_\epsilon^* \in (\bar{u}, 1/r_1)$ such that $R_c(u_\epsilon^*) = 0$.

For equation (45), we have the same argument as the proof of (b).$\square$

(d) From equation (38), if we consider $u \in (1/r_1, 2/\epsilon)$ then we have

$$P_\epsilon'(u) = \frac{2\epsilon^2u}{(r_1u-1)(r_2u-1)(4-\epsilon^2u^2)}\left\{-\frac{(r_1+r_2)(r_1r_2u^2)u-1}{(r_1u-1)(r_2u-1)} + \frac{4(1+r_1u)(1+r_2u)}{(4-\epsilon^2u^2)}\right\}. \tag{54}$$

Since $P_\epsilon'(\{1/r_1\}^+) < 0$, $P_\epsilon'(\{2/\epsilon\}^-) > 0$ and $P_\epsilon''(u) > 0$ for $u \in (1/r_2, 1/r_1)$, there is a $\hat{u} \in (1/r_1, 2/\epsilon)$ such that $P_\epsilon'(\hat{u}) = 0$ and $P_\epsilon(\hat{u})$ is a minimum value for $u \in (1/r_1, 2/\epsilon)$.

Since $P_\epsilon'(\hat{u}) = 0$, from equation (38), we have

$$\frac{(r_1 + r_2)(r_1 r_2 (\hat{u})^2 - 1)\hat{u}}{(r_1\hat{u} - 1)(r_2\hat{u} - 1)} = \frac{4(1 + r_1\hat{u})(1 + r_2\hat{u})}{(4 - \epsilon^2(\hat{u})^2)} \tag{55}$$

Therefore, from equation (55), we have

$$\begin{aligned} P_\epsilon(\hat{u}) &= \frac{(1 + r_1\hat{u})(1 + r_2\hat{u})}{(r_1\hat{u} - 1)(r_2\hat{u} - 1)} \left(\frac{\epsilon^2(\hat{u})^2}{4 - \epsilon^2(\hat{u})^2} \right) > 0 \\ &= \frac{4\epsilon^2\hat{u}(1 + r_1\hat{u})^2(1 + r_2\hat{u})^2}{(4 - \epsilon^2(\hat{u})^2)^2(r_1 + r_2)(r_1 r_2(\hat{u})^2 - 1)}, \end{aligned} \tag{56}$$

and we found the minimum value $P_\epsilon(\hat{u}) = \mathrm{O}(\epsilon^2)$. Therefore, $R_c(\hat{u}) = P_\epsilon(\hat{u}) - Q(\hat{u}) < 0$. Since $R_c((1/r_1)^+) > 0$, $R_c((2/\epsilon)^-) > 0$ and $R_c(\hat{u}) < 0$, there are at least two root $u_2 \in (1/r_1, \hat{u})$ and $u_3 \in (\hat{u}, 2/\epsilon)$ such that $R_c(u_2) = R_c(u_3) = 0$. $\square$

5.2. Phase-Planes for Model C

Next, we find the eigenvalues λ satisfy the following equation

$$\lambda^2 + \frac{\alpha c}{lu}\lambda - (-1 - k_3\frac{\partial C_1}{\partial u}) = 0, \tag{57}$$

$$\text{where } C_1 = \frac{\ln(P_\epsilon(u))}{u}. \tag{58}$$

Hence,

$$\frac{\partial C_1}{\partial u} = \frac{\partial[\ln(P_\epsilon(u))/u]}{\partial u} = -\frac{\ln P_\epsilon(u)}{u^2} + \frac{1}{uP_\epsilon(u)}\frac{\partial(P_\epsilon(u))}{\partial u}. \tag{59}$$

Thus, from equation (57), we have

$$\lambda = \frac{\alpha c}{2lu}\left\{-1 \pm \sqrt{1 - 4\left(\frac{\alpha u}{lc}\right)^2\left(1 + k_3\frac{\partial C_1}{\partial u}\right)}\right\}. \tag{60}$$

Let $\Delta = 1 - 4\left(1 + k_3 \frac{\partial C_1}{\partial u}\right)\left(\frac{lu}{\alpha c}\right)^2$, then we have three possible cases :

Case 1: If $\Delta < 0$, then two eigenvalues $\lambda_{1,2} = -a \pm b\mathrm{i}$ for $a, b > 0$, so the fixed point is a stable spiral point.

Case 2: If $0 < \Delta < 1$, then two eigenvalues are negative, so the fixed point is a stable node.

Case 3: If $\Delta > 1$, then one eigenvalue is positive and the other is negative, so the fixed point is a saddle point.

Theorem 5.2

(a) The fixed point, $u_{\epsilon *} = \frac{1}{r_2} + \mathrm{O}(\epsilon^2)$ is a saddle point.

(b) The fixed point, $u_\epsilon^* = \frac{1}{r_1} + \mathrm{O}(\epsilon^2)$ is a stable spiral point.

Proof :

Since fixed point (u, v) satisfy equation (41), from equation (59), we have

$$\begin{aligned} & 1 + k_3 \frac{\partial C_1}{\partial u} \\ & = 1 + k_3 \left\{ -\frac{\ln P_\epsilon(u)}{u^2} - \frac{2(r_1 + r_2)(1 - r_1 r_2 u^2)}{u(1 - r_1^2 u^2)(r_2^2 u^2 - 1)} + \frac{8}{u^2(4 - \epsilon^2 u^2)} \right\} \\ & = 2 - \frac{k_2}{u} - \frac{2k_3(r_1 + r_2)(1 - r_1 r_2 u^2)}{u(1 - r_1^2 u^2)(r_2^2 u^2 - 1)} + \frac{8k_3}{u^2(4 - \epsilon^2 u^2)}. \end{aligned} \tag{61}$$

In order to know which case it should be for different fixed point, we further calculate:

$$\begin{aligned} \Delta &= 1 - 4\left(1 + k_3 \frac{\partial C_1}{\partial u}\right)\left(\frac{lu}{\alpha c}\right)^2, \\ &= 1 - 4\left(2 - \frac{k_2}{u} - \frac{2k_3(r_1 + r_2)(1 - r_1 r_2 u^2)}{u(1 - r_1^2 u^2)(r_2^2 u^2 - 1)} + \frac{8k_3}{u^2(4 - \epsilon^2 u^2)}\right)\left(\frac{lu}{\alpha c}\right)^2, \\ &= 1 - 8\left(\frac{lu}{\alpha c}\right)^2 + \left(\frac{4k_2 l^2 u}{\alpha^2 c^2}\right) + \frac{8k_3 l^2 u(r_1 + r_2)(1 - r_1 r_2 u^2)}{\alpha^2 c^2(1 - r_1^2 u^2)(r_2^2 u^2 - 1)} - \frac{32 k_3 l^2}{\alpha^2 c^2(4 - \epsilon^2 u^2)}. \end{aligned} \tag{62}$$

(a) We consider the fixed point, $u_{\epsilon *} = \frac{1}{r_2} + \mathrm{O}(\epsilon^2)$. Since the fourth term of equation

(62) is positive with magnitude $\mathrm{O}(1/\epsilon^2)$ and other terms are bounded , thus $\Delta > 1$ and the fixed point $u_{\epsilon *} = \frac{1}{r_2} + \mathrm{O}(\epsilon^2)$ is a saddle point. □

(b) We consider the fixed point, $u_\epsilon^* = \frac{1}{r_1} + \mathrm{O}(\epsilon^2)$. Since the fourth term of equation (62) is negative with magnitude $\mathrm{O}(1/\epsilon^2)$ and other terms are bounded , thus $\Delta < 0$ and the fixed point $u_\epsilon^* = \frac{1}{r_2} + \mathrm{O}(\epsilon^2)$ is a stable spiral point. □

The solution curves on the $u - v$ phase plane are shown in Figure 4(a)-(d), where we set $k_2 = 0.1$, $M_b = 0.5$ and $\epsilon = 10^{-3}$. In Figure 4(a), there are two vertical dotted lines, the left one is $u = 1/r_2$ and the right one is $u = 1/r_1$, which divide the $u - v$ plane into three regions. Figure 4(b) is the detail for the region near the line of $u = 1/r_2$ in Figure 4(a), which make it possible to see the fine structures. We can see that there is one center and one saddle point near the dotted line $u = 1/r_2$. Figure 4(c) is the detail for the region near the line of $u = 1/r_1$ in Figure 4(a). We can see that there is one spiral point and one saddle point near the dotted line $u = 1/r_1$. Figure 4(d) is a closer-looking of the spiral point in the region of $u > 1/r_1$.

These figures reconfirm the analytic results and also make the behavior of the solution curve clear.

6. Conclusions

We have studied the properties of solution curves on the phase plane of dynamical systems of planet-belt interaction by the standard fixed-point analysis.

The system is divided into three regions: (a) the region between the central star and the inner edge of the belt, (b) the region out of the outer edge of the belt, (c) the region between the inner edge and the outer edge of the belt. The dynamics in three regions are governed by three different models and the planet moves around these regions.

We analytically prove some properties of the system and also show some bifurcation diagrams of fixed points for different cases: the number and properties of fixed points changed with the values of parameters k_2 and M_b in general.

Our analytical and numerical results show that, in most cases, the locations of fixed points depend on the values of these parameters and these fixed points are either center (structurally stable) or saddle (unstable).

On the other hand, we found that there are two special fixed points: one is on the inner and another is on the outer edges of the belt. The one on the inner edge is a stable focus (asymptotically stable) and the one on the outer edge is a saddle (unstable).

This interesting result is consistent with the observational picture of Asteroid Belt between the Mars and Jupiter: the Mars is moving stablely close to the inner edge but the Jupiter is quite far from the outer edge.

REFERENCES

Chan, H.S.Y. & Chung, K.W. and Dongwen, Qi [2001] "Some bifurcation diagrams for limit cycles of Quadratic differential systems", Int. J. Bifurcation and Chaos **11**, 197-206.

Clausen, S. & Helgesen, G. and Skjeltorp, A.T. [1998] "Braid description of few body dynamics", Int. J. Bifurcation and Chaos **7**, 1383-1397.

Goldstein, H. [1980] "Classical Mechanics", Addison-Wesley Publishing Company

Jiang, I.-G. & Ip, W.-H. [2001] "The planetary system of upsilon Andromedae", Astronomy & Astrophysics **367**, 943-948.

Kaulakys, B. & Ivanauskas, F. and Meskauskas, T. [1999] "Synchronization of chaotic systems driven by identical noise", Int. J. Bifurcation and Chaos **9**, 533-539.

Thommes, E.W. & Duncan, M.J. and Levison, H.F. [1999] "The formation of Uranus and Neptune in the Jupiter-Saturn region of the Solar System", Nature **402**, 635-638

Yeh, L.-C. & Jiang, I.-G. [2001] "Orbital Evolution of Scattered Planets", The Astrophysical Journal **561**, 364-371.

This manuscript was prepared with the AAS LaTeX macros v4.0.

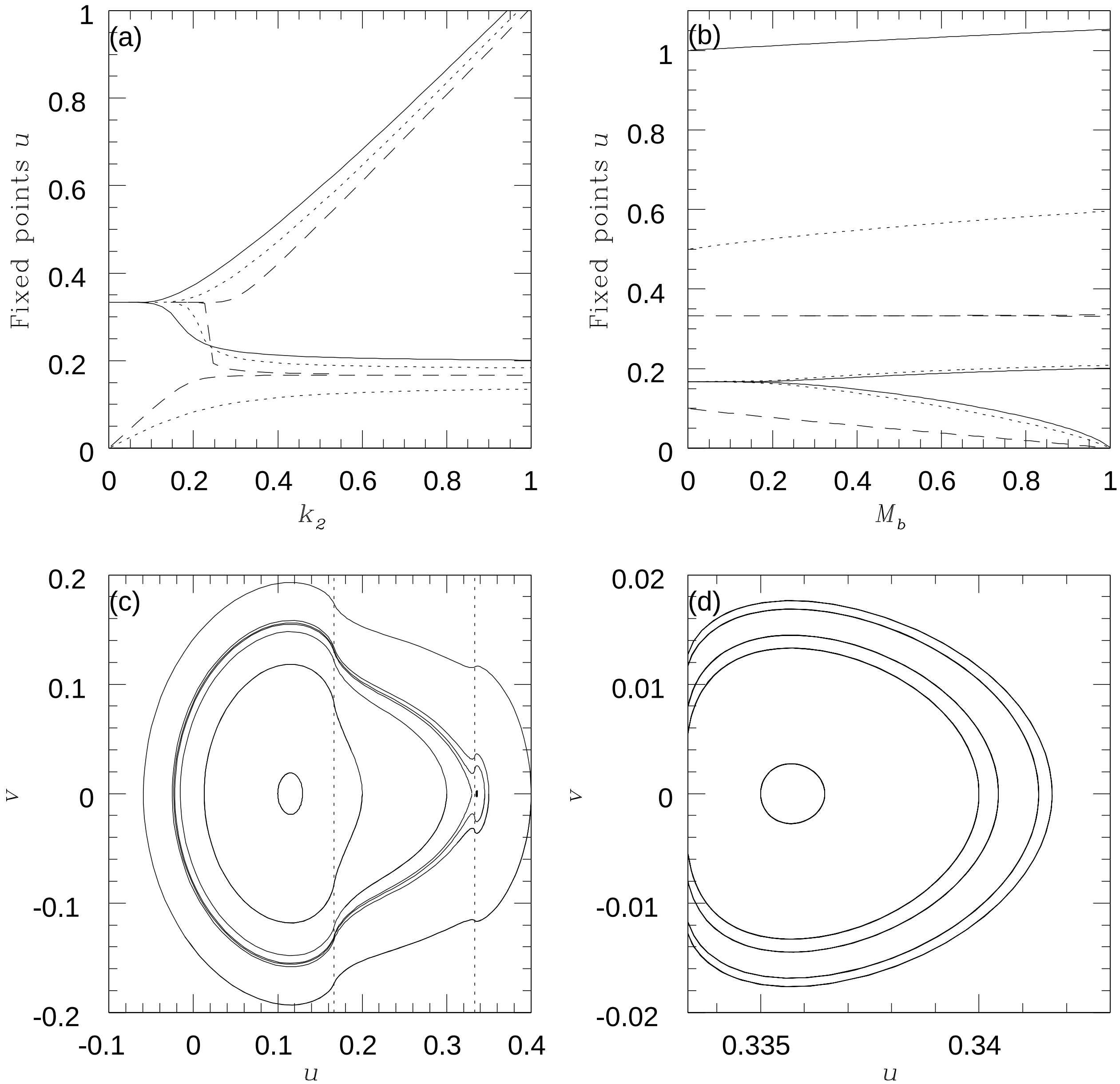

Fig. 1.— Bifurcation diagrams of fixed points and phase planes for Model A with $r_1 = 3$, $r_2 = 6$. (a) The bifurcation diagram of fixed points on $k_2 - u$ plane, where dashed lines are for $M_b = 0.1$, dotted lines are for $M_b = 0.5$ and solid lines are for $M_b = 1.0$. (b) The bifurcation diagram of fixed points on $M_b - u$ plane, where dashed lines are for $k_2 = 0.1$, dotted lines are for $k_2 = 0.5$ and solid lines are for $k_2 = 1.0$. (c) The solution curves on the $u - v$ plane, where we set $k_2 = 0.2$, $M_b = 0.3$. There are two vertical dotted lines, the left one is $u = 1/r_2$ and the right one is $u = 1/r_1$. (d) The detail near the rightest fixed points

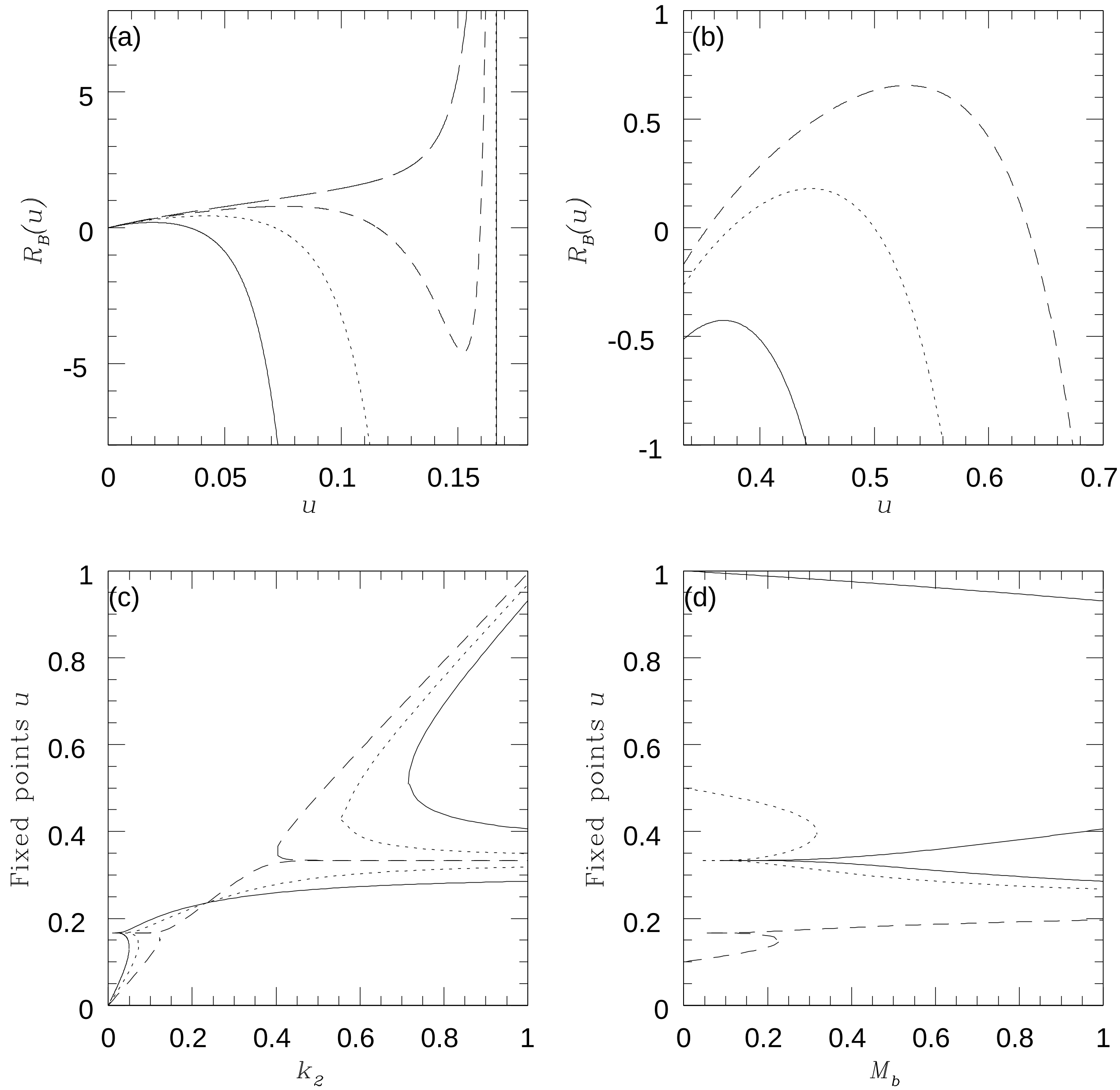

Fig. 2.— Bifurcation diagrams of fixed points for Model B with $r_1 = 3$, $r_2 = 6$. (a) R_B as a function of u for the cases that $M_b = 0.5$ and $k_2 = 0.02$ (solid line), $k_2 = 0.04$ (dotted line), $k_2 = 0.06$ (dashed line), $k_2 = 0.08$ (long dashed line). (b) R_B as a function of u for the cases that $M_b = 0.5$ and $k_2 = 0.4$ (solid line), $k_2 = 0.5$ (dotted line), $k_2 = 0.6$ (dashed line). (c) The fixed points on $k_2 - u$ plane, where dashed lines are for $M_b = 0.1$, dotted lines are for $M_b = 0.5$ and solid lines are for $M_b = 1.0$. (d) The fixed points on $M_b - u$ plane, where dashed lines are for $k_2 = 0.1$, dotted lines are for $k_2 = 0.5$ and solid lines are for $k_2 = 1.0$.

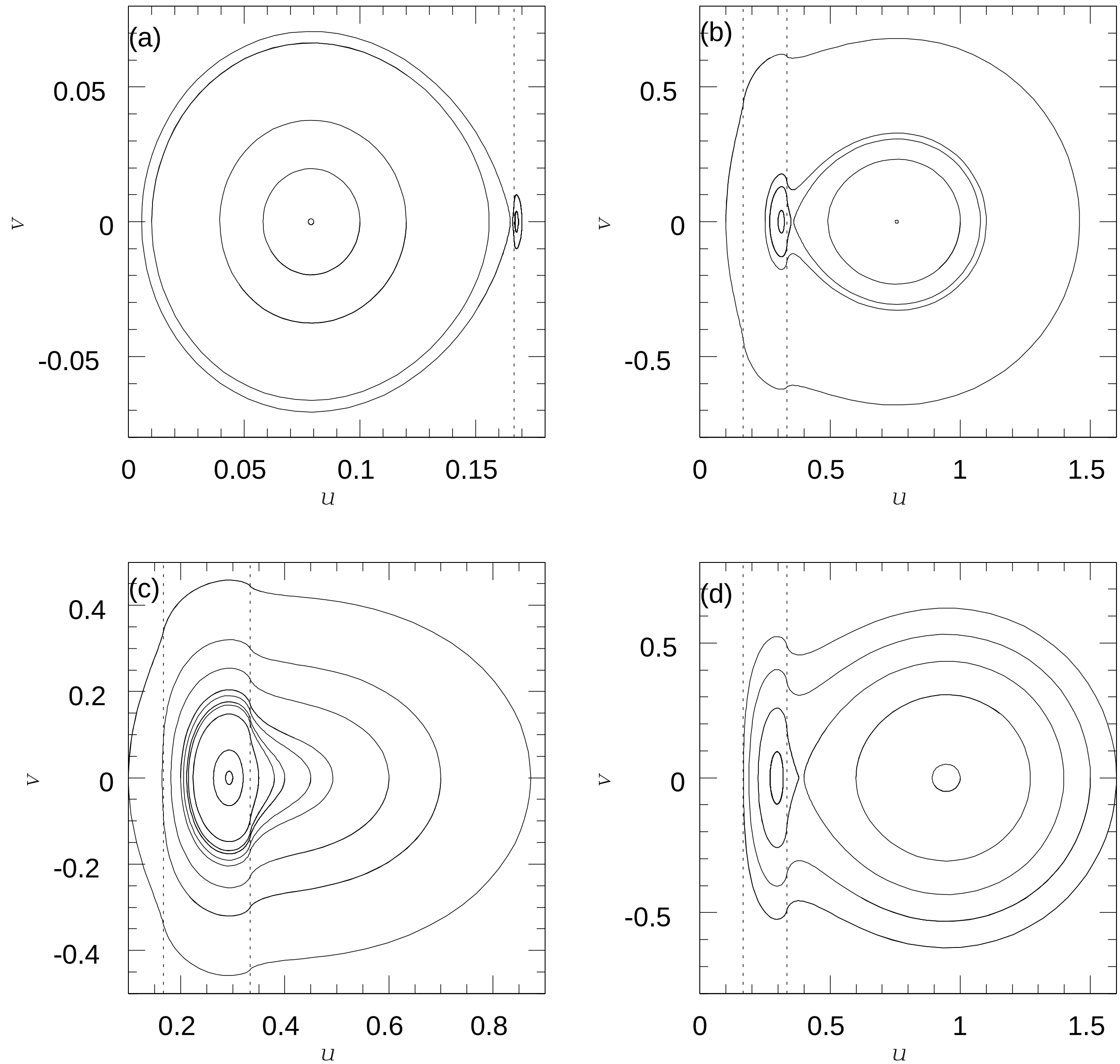

Fig. 3.— The phase planes for Model B with $r_1 = 3$, $r_2 = 6$. (a) The solution curves on the $u-v$ plane when $k_2 = 0.05$, $M_b = 0.5$. The vertical dotted line is $u = 1/r_2$. (b) The solution curves on the $u-v$ plane when $k_2 = 0.8$, $M_b = 0.5$. The left vertical dotted line is $u = 1/r_2$ and the right vertical dotted line is $u = 1/r_1$. (c) The solution curves on the $u-v$ plane when $k_2 = 0.5$, $M_b = 0.5$. The left vertical dotted line is $u = 1/r_2$ and the right vertical dotted line is $u = 1/r_1$. (d) The solution curves on the $u-v$ plane when $k_2 = 1.0$, $M_b = 0.8$. The left vertical dotted line is $u = 1/r_2$ and the right vertical dotted line is $u = 1/r_1$.

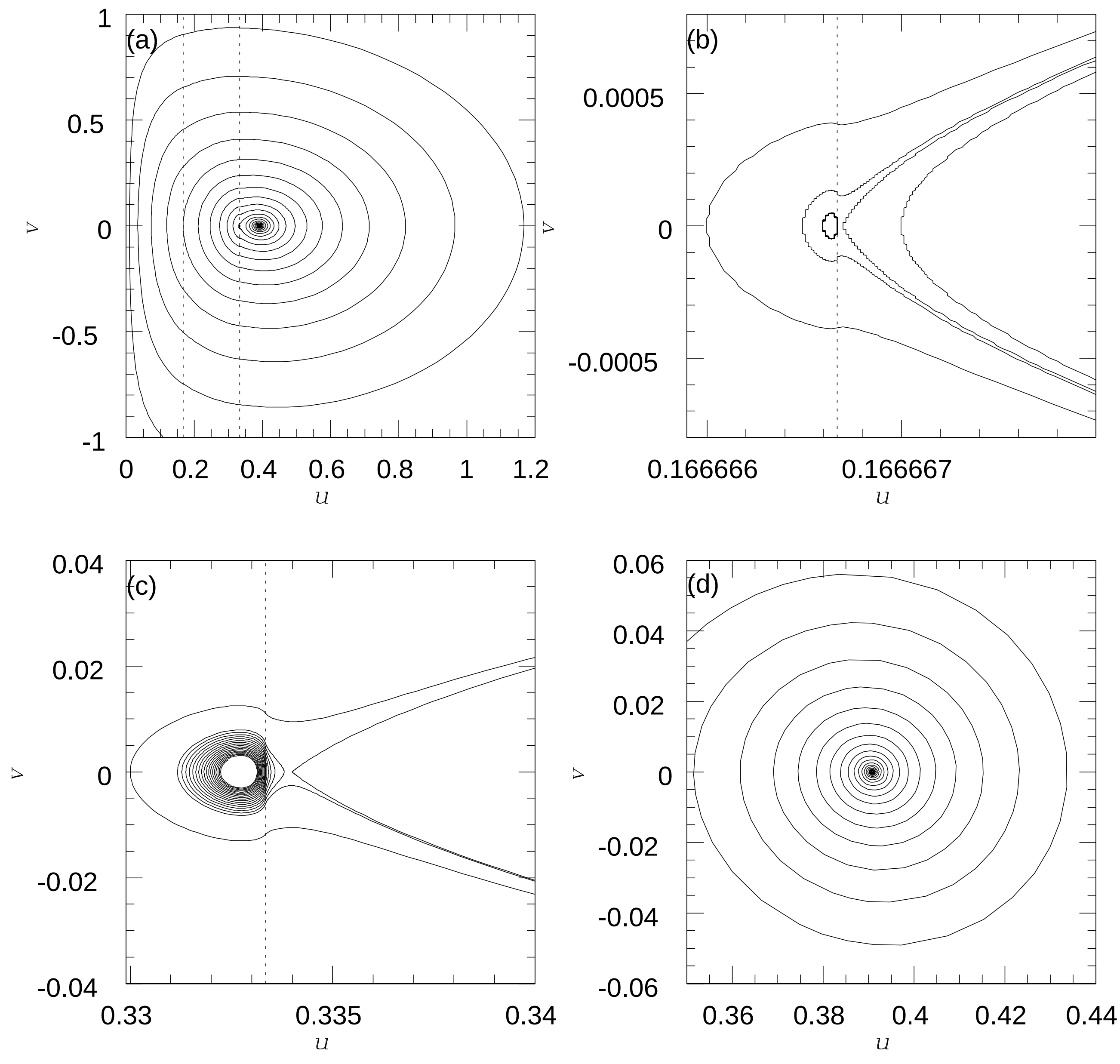

Fig. 4.— The phase planes for Model C when $r_1 = 3$, $r_2 = 6$, $k_2 = 0.1$, $M_b = 0.5$ and $\epsilon = 10^{-3}$. (a) The $u - v$ phase plane, the left vertical line is $u = 1/r_2$ and the right one is $u = 1/r_1$. (b) The detail for the region near the line of $u = 1/r_2$ in (a). (c) The detail for the region near the line of $u = 1/r_1$ in (a). (d) A closer-looking of the focus point in the region of $u > 1/r_1$.